

Charge radius and dipole response of ^{11}Li

H. Esbensen,¹ K. Hagino,² P. Mueller,¹ and H. Sagawa³

¹*Physics Division, Argonne National Laboratory, Argonne, Illinois 60439, USA*

²*Department of Physics, Tohoku University, Sendai, 980-8578, Japan*

³*Center for Mathematical Sciences, University of Aizu, Aizu-Wakamatsu, Fukushima 965-8560, Japan*

(Dated: November 12, 2018)

We investigate the consistency of the measured charge radius and dipole response of ^{11}Li within a three-body model. We show how these observables are related to the mean square distance between the ^9Li core and the center of mass of the two valence neutrons. In this representation we find by considering the effect of smaller corrections that the discrepancy between the results of the two measurements is of the order of 1.5σ . We also investigate the sensitivity to the three-body structure of ^{11}Li and find that the charge radius measurement favors a model with a 50% s-wave component in the ground state of the two-neutron halo, whereas the dipole response is consistent with a smaller s-wave component of about 25% value.

PACS numbers: 21.10.Ft, 21.45.+v, 21.60.Gx, 25.60.-t

INTRODUCTION

The properties of the two-neutron halo nucleus ^{11}Li have been discussed in numerous theoretical and experimental papers but knowledge about its structure is still uncertain. In the past year, the results of two important measurements have been published, namely, the RMS (root-mean-square) charge radius of ^{11}Li obtained from laser spectroscopy [1] and the dipole response, which was probed by Coulomb dissociation on a Pb target [2]. The purpose of this paper is to investigate whether the two measurements can be explained simultaneously within a three-body model and to see what are the implications of the two results for the structure of ^{11}Li .

The nucleus ^{11}Li is an excellent example of a so-called borromean system, a bound three-body system in which none of the two-body subsystems form a bound state. Thus ^{11}Li can be viewed as a three-body system consisting of a ^9Li core and two valence neutrons where neither ^{10}Li nor the dineutron system has a bound state. The nucleus ^{11}Li has only one bound state with a two-neutron separation energy of about 300 keV.

Theoretical studies of ^{11}Li have primarily been based on three-body models of the two valence neutrons interacting with the ^9Li core, and it has been a major challenge over the past 10–15 years to obtain information about the neutron-core interaction, i. e., about the scattering states in the unbound nucleus ^{10}Li . Early studies [3] assumed a dominant p-wave structure of the two-neutron halo, based on a rather high-lying p-wave resonance in ^{10}Li . Another model [4] assumed a shallow neutron-core potential, which does not have any bound states, and this resulted in a strongly s-wave dominated ground state of the two-neutron halo. In order to explore the structure of ^{11}Li , a wider range of models were developed [5] and compared to measurements.

A better calibration of three-body models for ^{11}Li became possible with an accurate measurement of the two-

neutron separation energy, $S_{2n} = 295 \pm 15$ keV [6], and a production measurement [7] which probed the continuum of ^{10}Li . The latter measurement suggested a p-wave resonance at about 540 keV and some influence of s-wave scattering near threshold. Let us also mention that the quadrupole moments of ^9Li and ^{11}Li are the same within the 15% experimental uncertainty [8]; this can be taken as a justification for using three-body models.

An analysis of the β -decay of ^{11}Li [9] showed that about 45–55 % of the two-neutron halo must be in $p_{1/2}$ orbits, whereas the remaining part would most likely occupy s-waves. Analyses of the momentum distributions produced in high-energy breakup reactions also suggested a large s-wave component, from 20–40 % [10] to 35–55 % [11]. In fact, there seems to be a consensus toward a large s-wave component in two-neutron ground state, a component that is much larger than what was expected. This feature may be related to the famous parity inversion in the neighboring nucleus ^{11}Be , where the ground state is a $1/2^+$ state and not a $1/2^-$ state as one naively would expect for a p-shell nucleus. It is of interest to see how the recent charge radius [1] and dipole response [2] measurements fit into this trend.

THREE-BODY MODEL INTERPRETATION

There is a very close relationship within a three-body model between the charge radius and the dipole response of a two-neutron halo since they are both probes of the distance between the ^9Li core and the center-of-mass of the dineutron system. The mean square charge radius $\langle r_p^2(Z, A) \rangle$ for point-nucleons, for example, can be expressed in terms of the charge radius of the core nucleus as follows,

$$\langle r_p^2(Z, A) \rangle = \langle r_p^2(Z, A-2) \rangle + \left(\frac{2}{A}\right)^2 \langle r_{c,2n}^2 \rangle, \quad (1)$$

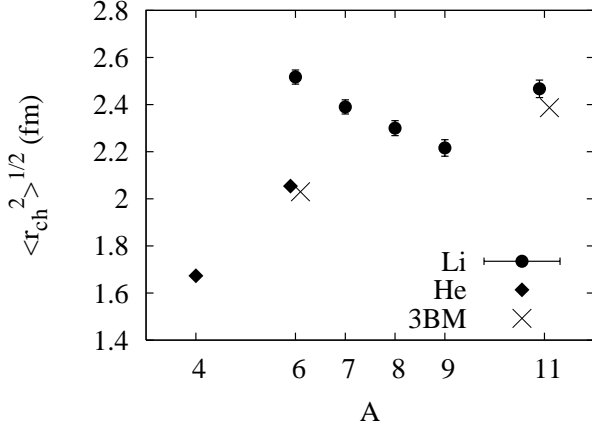


FIG. 1: Measured charge radii of He [15] and Li [1, 16] isotopes are compared to the predictions of the three-body models (3BM) of ${}^6\text{He}$ and ${}^{11}\text{Li}$ discussed in Ref. [14].

where the second term is the correction which is caused by the center of mass motion of the core nucleus in the presence of the two valence neutrons. The correction is proportional to the mean square distance, $\langle r_{c,2n}^2 \rangle$, between the core and the center of mass of the dineutron system.

The total strength of the dipole response of a two-neutron halo nucleus is approximately given by the cluster sum rule [3],

$$B(E1) = \frac{3}{4\pi} \left(\frac{Ze}{A} \right)^2 4 \langle r_{c,2n}^2 \rangle, \quad (2)$$

which is also expressed in terms of the mean square distance, $\langle r_{c,2n}^2 \rangle$, between the core and the dineutron system. The sum rule assumes that the total dipole strength can be calculated by closure, which includes dipole transitions to the Pauli blocked core states. The effect of Pauli blocking is a minor but not insignificant correction, as we discuss in the next section. However, if we ignore it, we see that the charge radius and dipole response measurements are closely related, since they are both probes of the core-dineutron distance.

To make contact with the measured charge radius r_{ch} we must correct the point-proton charge radii of Eq. (1) for the finite sizes of protons and neutrons. We should also consider the so-called Darwin-Foldy contribution and the effect of the spin-orbit charge density discussed in Ref. [12]. We therefore have the expression,

$$\langle r_{ch}^2 \rangle = \langle r_p^2 \rangle + \langle R_p^2 \rangle + \frac{A-Z}{Z} \langle R_n^2 \rangle + \frac{3\hbar^2}{4(mc)^2} + \langle r^2 \rangle_{so}, \quad (3)$$

where $\langle R_p^2 \rangle = 0.757(14) \text{ fm}^2$ and $\langle R_n^2 \rangle = -0.1161(22) \text{ fm}^2$ are the mean square charge radii of protons and neutrons [13], respectively, and $3\hbar^2/[4(mc)^2]$ is the Darwin-Foldy term.

TABLE I: The measured charge radius of ${}^6\text{He}$ [15], the change in the mean square charge radius of ${}^{11}\text{Li}$ and ${}^9\text{Li}$, and the mean square distance between the ${}^4\text{He}$ core and the two-neutron halo in ${}^6\text{He}$ are compared to results of three-body models (3BM) and GFMC calculations. The spin-orbit correction, Eq. (5), was ignored and the charge radius of ${}^4\text{He}$ was set to $1.673(1) \text{ fm}$.

Nucleus	$\langle r_{ch}^2 \rangle^{1/2} \text{ (fm)}$	$\delta \langle r_{ch}^2 \rangle \text{ (fm}^2\text{)}$	$\langle r_{c,2n}^2 \rangle \text{ (fm}^2\text{)}$
${}^6\text{He}$ exp. [15]	2.054(14)	1.42(5)	13.8 ± 0.5
3BM [14]	2.036	1.35	13.2
3BM [17]	2.011	1.25	12.3
GFMC [18]	2.08(4)	1.49(15)	14.5 ± 1.5

Inserting Eq. (1) into Eq. (3) we obtain the following expression for the difference between the mean square charge radii of the two-neutron halo nucleus and the core nucleus,

$$\begin{aligned} \delta \langle r_{ch}^2 \rangle &= \langle r_{ch}^2(Z, A) \rangle - \langle r_{ch}^2(Z, A-2) \rangle \\ &= \left(\frac{2}{A} \right)^2 \langle r_{c,2n}^2 \rangle - \frac{0.232}{Z} + \langle r^2 \rangle_{2n}^{so}. \end{aligned} \quad (4)$$

It is seen that the proton charge radius R_p in Eq. (3) drops out of Eq. (4), and so does the constant Darwin-Foldy term. The only two corrections that survive, $-0.232/Z$ and $\langle r^2 \rangle_{2n}^{so}$, are due to the non-zero, mean square charge radius of a neutron and the spin-orbit charge density of the two valence neutrons.

In the following we ignore the spin-orbit correction to the charge radius except when otherwise explicitly stated. The reason is that this correction is model dependent, so it is not obvious how one should convert the measured isotope shift into a mean square, core-dineutron distance. One can calculate the spin-orbit correction in different models from the explicit expressions that are given in Ref. [12]. In the shell model for spherical nuclei, with two valence neutrons occupying an unfilled (l, j) sub-shell, the spin-orbit correction is

$$\langle r^2 \rangle_{2n}^{so} = \frac{2\mu_n}{Z} \left(\frac{\hbar}{m} \right)^2 \langle \mathbf{l} \cdot \mathbf{s} \rangle, \quad (5)$$

where $\mu_n = -1.913$ in the neutron magnetic moment, m is the neutron mass, and

$$\langle \mathbf{l} \cdot \mathbf{s} \rangle = j(j+1) - l(l+1) - 3/4.$$

In three-body models one would have to calculate $\langle \mathbf{l} \cdot \mathbf{s} \rangle$ numerically as an average value, since the 0^+ ground state of the two-neutron halo contains many (l, j) single-particle components [14].

We show in Fig. 1 the measured RMS charge radii for the helium [15] and lithium [1, 16] isotopes. The results for ${}^6\text{He}$ and ${}^{11}\text{Li}$ are compared with the three-body

model calculations of Ref. [14]. These calculations employed a density-dependent contact interaction to simulate low-energy nn scattering, and the ${}^4\text{He}$ -neutron Hamiltonian was calibrated to reproduce the known low-energy neutron- α scattering phase shifts. The calculations for ${}^{11}\text{Li}$ are discussed below.

The measured charge radius of ${}^6\text{He}$ and the mean-square, core-dineutron distance we obtain when we ignore the spin-orbit correction in Eq. (4) are compared in Table I to the results of different models, namely, two three-body models of Refs. [14, 17], and a recent GFMC (Greens function Monte Carlo) calculation [18]. The latter is an improvement over the results that were published in Ref. [19].

Let us estimate the spin-orbit correction to the ${}^6\text{He}$ - ${}^4\text{He}$ mean-square charge radius difference in the extreme limit where the valence neutrons occupy a pure $(p_{3/2})^2$ configuration. Then $\langle \mathbf{l} \cdot \mathbf{s} \rangle = 1$, and we obtain from Eq. (5) the correction $\langle r^2 \rangle_{2n}^{\text{so}} = -0.085 \text{ fm}^2$. Another estimate is to evaluate the average spin-orbit correction in the three-body model developed in Ref. [14], since we know in this case the occupation probabilities of the single-particle orbits. The model quoted in line 5, Table II of Ref. [14], has 83% of the two-neutron halo in $(p_{3/2})^2$ orbits. Considering all orbits of the halo we obtain the average value $\langle \mathbf{l} \cdot \mathbf{s} \rangle = 0.82$. This implies the spin-orbit correction $\langle r^2 \rangle_{2n}^{\text{so}} = -0.07 \text{ fm}^2$, which would bring the GFMC calculation into perfect agreement with the measurement, whereas the three-body model [14] would be off by 10%, which is a discrepancy of almost 3σ .

The discrepancy between the measured and calculated charge radius of ${}^{11}\text{Li}$ which can be seen in Fig. 1 may reflect uncertainties in the neutron-core Hamiltonian that we have used. The neutron halo ground state contains in this case 23% s-waves and is therefore referred to as the $s23$ model below. The model Hamiltonian [14] was calibrated to reproduce the measured two-neutron separation energy [6] and also the p-wave resonance structure observed in Ref. [7], but there is still some uncertainty in the s-wave strength which we explore below.

DIPOLE RESPONSE

The measured dipole strength distribution [2] is compared in Fig. 2A to the prediction of an old three-body model of ${}^{11}\text{Li}$ [20]. The calculated distributions include the effect of the experimental energy resolution [2]. Although this model has a rather small two-neutron separation energy of 200 keV and did not include the recoil effects in a three-body system, it was able to reproduce fragmentation data at 800 MeV/nucleon fairly well [21], and Fig. 2A shows that it also produces a dipole response that is in surprisingly good agreement with the measurement [2]. The strong peak near 300–400 keV (solid curve) is produced by the strong attractive interaction between

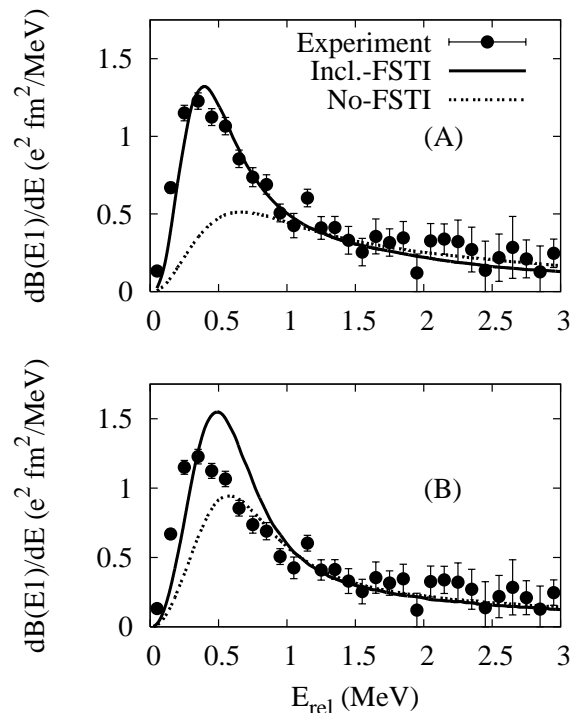


FIG. 2: The measured dipole response of ${}^{11}\text{Li}$ [2] is compared (A) to the calculations of Ref. [20], with (solid) and without (dashed) the effect of the final state nn interaction, and (B) to calculations that are based on the $s23$ model described in the text.

the neutrons in the final state. If this final state interaction is set to zero we obtain the dashed curve.

The measured dipole strength distribution [2] is compared in Fig. 2B to new calculations that are based on the $s23$ model [14]. The calculations (with and without the effect of the final state nn interaction) include the experimental energy resolution as done in Ref. [2]. The ground state of the $s23$ model has a realistic two-neutron separation of 295 keV and includes recoil effects in the three-body system exactly, c. f. the last term of Eq. (3.1) in Ref. [14]. The recoil effects are treated approximately in the three-body final state of the dipole response by ignoring the off-diagonal component $\vec{p}_1 \cdot \vec{p}_2 / (A_c m)$ (the last term in Eq. (3.3) of Ref. [14]), whereas the diagonal term $\vec{p}_1^2 / (2A_c m) + \vec{p}_2^2 / (2A_c m)$ is included through the reduced mass. With this approximation, the continuum dipole response can be computed with the method of Ref. [20]. We have checked the accuracy of this approximation with the discretized dipole strength function of Ref. [22] and have confirmed that the approximation works well for the ${}^{11}\text{Li}$ nucleus. The calculated peak (solid curve in Fig. 2B) is higher and shifted slightly toward higher energies in comparison to the data but the overall strength is very reasonable.

The total dipole strength that was measured up to a 3 MeV relative energy is $B(E1)_{\text{exp}} = 1.42 \pm 0.18$

TABLE II: The difference between the measured mean square charge radii of ^{11}Li and ^9Li [1], and the mean square distance between the ^9Li core and the two-neutron halo (extracted from Eq. (4) for $\langle r^2 \rangle_{2n}^{\text{so}}=0$), are compared to the results of three-body models (3BM), and the values extracted from the Coulomb dissociation (CD) experiment [2]. The assumed charge radius of ^9Li was 2.216(35) fm. The last column shows the mean square distance between the two valence neutrons.

Nucleus	$\delta\langle r_{ch}^2 \rangle$ (fm ²)	$\langle r_{c,2n}^2 \rangle$ (fm ²)	$\langle r_{n,n}^2 \rangle$ (fm ²)
^{11}Li exp [1]	1.175(124)	37.9 ± 3.7	
revised [23]	1.104(85)	35.7 ± 2.6	
Old 3BM [3]	0.728	24.35	39.0
s05 3BM [14]	0.541	18.7	42.8
s23 3BM [14]	0.789	26.2	45.9
s32 3BM new	0.895	29.4	51.6
s50 3BM [10]	1.120	36.2	70.1
CD exp. [2]	0.82(11)	27.2 ± 3.5	

e^2fm^2 . The calculated dipole strength up to 3 MeV, $B(E1, E_{\text{rel}} \leq 3 \text{ MeV})_{\text{cal}}$, is $1.26 \text{ e}^2\text{fm}^2$ in the old model (Fig. 2A) and $1.38 \text{ e}^2\text{fm}^2$ in the new $s23$ model (Fig. 2B). Since the measured and calculated dipole strengths shown in Fig. 2 do not differ much, it seems reasonable to estimate the mean-square, core-dineutron distance associated with the experiment by the simple scaling,

$$\langle r_{c,2n}^2 \rangle \approx \frac{B(E1, E_{\text{rel}} \leq 3 \text{ MeV})_{\text{exp}}}{B(E1, E_{\text{rel}} \leq 3 \text{ MeV})_{\text{cal}}} \langle r_{c,2n}^2 \rangle_{3\text{BM}}, \quad (6)$$

in terms of the mean-square distance $\langle r_{c,2n}^2 \rangle_{3\text{BM}}$ we obtain in the three-body model. We note that this scaling method is consistent with the cluster sum rule but it does not necessarily require that the total dipole strength of the model is given by the cluster sum rule. We emphasize that the calculated dipole strength, which we insert into Eq. (6), is calculated in a model that respects the Pauli principle, whereas the cluster sum rule does not.

The scaling method (6) gives essentially the same result independent of which of the two models we use (the old model or the new $s23$ model). The average value is shown in the last line of Table II and it represents the mean-square, core-dineutron distance we extract from the measured dipole strength distribution. The last line of Table II also gives the difference in the mean-square charge radius of ^{11}Li and ^9Li , which we derive from Eq. (4) by ignoring the spin-orbit correction.

We note that the RMS core-dineutron distance quoted in Ref. [2], which is $5.01 \pm 0.32 \text{ fm}$, is smaller than the 5.22 fm value we obtain from the last line of Table II. The smaller size is the result of identifying the estimated total dipole strength ($1.78 \text{ e}^2\text{fm}^2$) with the cluster sum rule, Eq. (2). An even smaller size was obtained in Ref. [23] by fitting the measured dipole strength distribution of Ref. [2], and identifying the total strength with the

cluster rule. The result (Eq. (20) of Ref. [23]) translates into an RMS core-dineutron distance of 4.73 fm .

From an experimental point of view, extreme care must be taken when determining the total dipole strength associated with excitations of the halo, and when translating this strength into the size of the halo. This cannot be done accurately without some theoretical guidance because the dipole strength can only be resolved at low excitation energies. Moreover, the cluster sum rule (2), which is sometimes used to determine the size of the halo, is not exact because it ignores the Pauli blocking of some of the final states as we discussed earlier. In the old three-body model of Refs. [3, 20], for example, the total strength obtained by numerically integrating the calculated dipole strength distribution is $1.57 \text{ e}^2\text{fm}^2$, whereas the cluster sum rule strength is $1.73 \text{ e}^2\text{fm}^2$. That implies that the total strength is reduced by 10% compared to the cluster sum rule because of Pauli blocking.

CHARGE RADIUS MEASUREMENT

The measured charge radius of ^{11}Li is $2.467(37) \text{ fm}$ [1]. We emphasize that the uncertainty in the measured charge radius is partly due to the absolute calibration of one of the isotopes (^7Li). The difference between the mean square charge radii for different isotopes is therefore much more accurately determined. This is a great advantage for our discussion of the halo because the mean square distance between the ^9Li core and the dineutron is directly related, according to Eq. (4), to the difference $\delta\langle r_{ch}^2 \rangle$ between the mean square charge radii of ^{11}Li and ^9Li . We have considered this feature in our determination of the uncertainties on the values of $\delta\langle r_{ch}^2 \rangle$ and $\langle r_{c,2n}^2 \rangle$ shown in Table II.

The change in the mean square charge radius from the reference nucleus ^7Li was obtained from the measured isotope shift $\delta\nu_{\text{IS}}^{\text{exp}}(A, 7)$ and the calculated so-called finite mass correction $\delta\nu_{\text{IS}}^{\text{MS}}(A, 7)$ according to the expression [1]

$$\langle r_{ch}^2(A) \rangle - \langle r_{ch}^2(7) \rangle = \frac{\delta\nu_{\text{IS}}^{\text{exp}}(A, 7) - \delta\nu_{\text{IS}}^{\text{MS}}(A, 7)}{1566.1 \text{ kHz}} \text{ fm}^2. \quad (7)$$

The finite mass corrections that were used in Ref. [1] have recently been reevaluated [23]. Combining these new corrections with the measured isotope shifts of Ref. [1] one obtains the ‘revised’ charge radius and core-dineutron distance shown in Table II. The important quantity to our discussion is the size of the halo which is here represented by $\langle r_{c,2n}^2 \rangle$. We see that the value we obtain from the Coulomb dissociation experiment is smaller than the values we obtain from the two interpretations [1, 23] of the charge radius measurement. The deviation is in both cases a 2σ discrepancy.

In Table II we also give the results we obtain in various three-body models of ^{11}Li , ranging from the ‘Old’

three-body model of Ref. [3] to the $s50$ model of Ref. [10], which gives a 50% s -wave component in the ground state of the two-neutron halo. It is seen that the $s50$ model is in agreement with the charge radius measurement [1], whereas the $s23$ model of Ref. [14] (with 23% s -waves in the halo ground state) is consistent with the CD experiment.

Let us finally estimate the spin-orbit correction, Eq. (5), which we have ignored so far when applying Eq. (4). In the extreme model, where the two valence neutrons occupy the $(p_{1/2})^2$ configuration, the value of $\langle \mathbf{l} \cdot \mathbf{s} \rangle$ is -2 , and from Eq. (5) we obtain $\langle r^2 \rangle_{2n}^{\text{so}} = 0.113 \text{ fm}^2$. In the $s23$ model, where 61% of the halo is in the $(p_{1/2})^2$ configuration, 23% are s -waves, and 16% are in higher (l, j) orbits, we obtain the average value $\langle \mathbf{l} \cdot \mathbf{s} \rangle = -1.09$ and $\langle r^2 \rangle_{2n}^{\text{so}} = 0.062 \text{ fm}^2$. Inserting this value into Eq. (4), together with the core-dineutron distance obtained from the Coulomb dissociation experiment (last line of Table II), we now obtain the corrected value $\delta \langle r_{ch}^2 \rangle_{\text{CD}} = 0.88(11) \text{ fm}^2$ for the difference between the mean square charge radius of ^{11}Li and ^9Li . This implies that the charge radius of ^{11}Li extracted from the Coulomb dissociation experiment is $2.41(4) \text{ fm}$, which is consistent with the directly measured value of $2.467(37) \text{ fm}$ [1].

The main part of the uncertainty in the charge radius of ^{11}Li stems from the uncertainty in the charge radius of ^9Li . A better representation of the discrepancy we obtain in our three-body-model interpretation of the measured charge radius and dipole response of ^{11}Li is the difference

$$\delta \langle r_{ch}^2 \rangle_{\text{exp}} - \delta \langle r_{ch}^2 \rangle_{\text{CD}} = 1.10(8) - 0.88(11) = 0.22(14) \text{ fm}^2. \quad (8)$$

This is the result we obtain when we adopt revised finite mass corrections of Ref. [23]. The discrepancy is now of the order of 1.5σ .

MATTER RADIUS

Also quoted in Table II is the calculated mean square distance between the two halo neutrons, $\langle r_{n,n}^2 \rangle$, in ^{11}Li . This quantity is not probed by the two experiments discussed above. It is seen that this distance increases dramatically when the magnitude of the ground state s -wave component increases.

The RMS matter radius, obtained from an analysis of interaction cross sections provides an additional constraint on the size of the halo. The mean square matter radius of a two-neutron halo nucleus is determined by the size of the halo and the core nucleus as follows

$$\begin{aligned} \langle r_m^2(Z, A) \rangle &= \frac{A-2}{A} \langle r_m^2(Z, A-2) \rangle \\ &+ \frac{2(A-2)}{A^2} \langle r_{c,2n}^2 \rangle + \frac{1}{2A} \langle r_{n,n}^2 \rangle. \end{aligned} \quad (9)$$

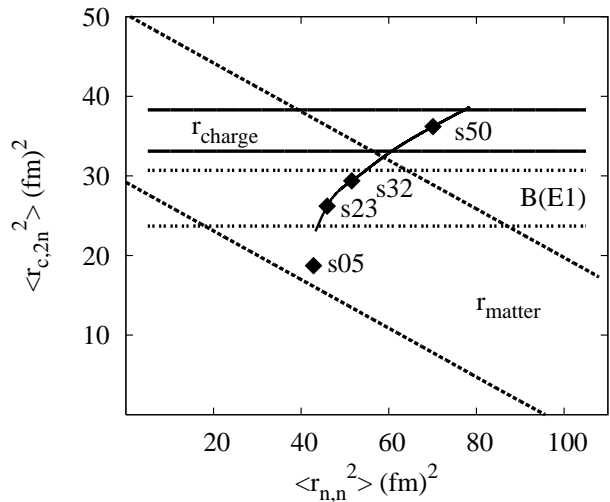


FIG. 3: Error bands on the size of the two-neutron halo in ^{11}Li obtained from the Coulomb dissociation experiment [2] ($B(E1)$), the charge radius [1] (r_{charge}), and the matter radius [24] (r_{matter}). The results obtained in three-body models, with 5 to 50% s -wave components, are indicated by diamonds.

The RMS radii obtained in Ref. [24] are 2.43 ± 0.02 and $3.27 \pm 0.24 \text{ fm}$, respectively, for ^9Li and ^{11}Li . From the halo distances given in Table II and the quoted matter radius of ^9Li we obtain a ^{11}Li RMS matter radius of 3.29 fm in the $s23$ model. Thus the $s23$ model agrees with the matter radius and also with the strength of the dipole response but the charge radius is too small compared with the measured value. The $s50$ model, on the other hand, agrees with the charge radius measurement, but the matter radius (which is 3.66 fm) and the dipole strength are too large compared to experiments.

The constraints on the mean square distances of the two-neutron halo obtained from the measurements of the charge radius, the dipole response, and the matter radius of ^{11}Li are illustrated in Fig. 3 together with the predictions of the three-body models. The limits from the charge radius are based on the revised values [23] in Table II and do not include the correction from the spin-orbit charge density. That correction may reduce the charge radius limits on $\langle r_{c,2n}^2 \rangle$ by 1.9 fm^2 , according to Eq. (4), if we adopt the spin-orbit correction $\langle r^2 \rangle_{2n}^{\text{so}} = 0.062 \text{ fm}^2$, which we obtained in the $s23$ model.

There is unfortunately some disagreement about the value of the matter radius which has been extracted from reaction data. An example is Ref. [25] where RMS radii of 2.30 and $3.53 \pm 06 \text{ fm}$ were obtained for ^9Li and ^{11}Li , respectively. This constraint provides a lower limit which is close to the upper limit of the matter radius shown in Fig. 3, and it would therefore favor the $s50$ over the $s23$ model. However, we do not think this is a reasonable solution because the $s50$ model produces a dipole response that has roughly a 33% larger strength than what has

been observed (compare the values of $\langle r_{c,2n}^2 \rangle$ shown in Table II).

FINAL REMARKS

We think that the 1.5σ discrepancy we obtain in our three-body model interpretation of the measured charge radius and dipole response of ^{11}Li is most likely caused by the neglect of core polarization. Actually, it may seem surprising that the effect of core polarization is not much more dramatic.

In order to estimate the effect of core polarization, we have performed Skyrme Hartree-Fock calculations for ^9Li and ^{11}Li using the filling approximation and the SGII interaction. The results show that the mean-square charge radius of ^{11}Li increases by 0.3 fm^2 from that of ^9Li because of the core polarization effect, which is caused by the proton-neutron interaction when the valence neutrons occupy p-waves, whereas it increases by about 0.2 fm^2 for s-waves. This accounts roughly for the discrepancy, Eq. (8), between the charge radius and the Coulomb dissociation experiment.

We conclude that it would be desirable to extend the three-body model so that one can consider the effect of core polarization in a consistent way. Work in this direction has already been done for the ground state of ^{11}Li [26], and it is also being pursued by other groups [27]. The work by Varga et al. [26] shows that core polarization does play a significant role in their microscopic cluster model calculation of the charge radius of ^{11}Li . This can be seen in Fig. 2 of Ref. [1], where their results, with and without the effect of core polarization, are compared to the measured charge radius. A further test of such models is provided by the measured quadrupole moments of ^9Li and ^{11}Li [8], and by the dipole response that was extracted from Coulomb dissociation data [2]. In this connection, it would also be very useful to test the consistency of the measured charge radius and dipole response of ^6He because the effect of core polarization should be much smaller for an α core.

We are grateful to T. Nakamura for including the experimental energy resolution in the calculated dipole response, and to S. Shlomo and S. C. Pieper for reminding us of the significance of the spin-orbit charge density. This work was supported (H.E. and P.M.) by the

U.S. Department of Energy, Office of Nuclear Physics, under Contract No. DE-AC02-06CH11357, and (K.H.) by the Grant-in-Aid for Scientific Research, Contract No. 19740115 from the Japanese Ministry of Education, Culture, Sports and Technology.

-
- [1] R. Sanchez *et al.*, Phys. Rev. Lett. **96**, 033002 (2006).
 - [2] T. Nakamura *et al.*, Phys. Rev. Lett. **96**, 252502 (2006).
 - [3] G. F. Bertsch and H. Esbensen, Ann. Phys. **209**, 327 (1991).
 - [4] M. V. Zhukov *et al.*, Phys. Lett. B **265**, 19 (1991).
 - [5] I. J. Thompson and M. V. Zhukov, Phys. Rev. C **49**, 1904 (1994).
 - [6] B. M. Young *et al.*, Phys. Rev. Lett. **71**, 4124 (1993).
 - [7] B. M. Young *et al.*, Phys. Rev. C **49**, 279 (1994).
 - [8] D. Borremans *et al.*, Phys. Rev. C **72**, 044309 (2005).
 - [9] T. Suzuki and T. Otsuka, Phys. Rev. C **56**, 847 (1997).
 - [10] G. F. Bertsch, K. Hencken and H. Esbensen, Phys. Rev. C **57**, 1366 (1998).
 - [11] H. Simon *et al.*, Phys. Rev. Lett. **83**, 496 (1999).
 - [12] J. L. Friar and J. W. Negele, Adv. Nucl. Phys. **8**, 219 (1975).
 - [13] Particle Data Group, S. Eidelman *et al.*, Phys. Lett. B **592**, 1 (2004).
 - [14] H. Esbensen, G. F. Bertsch and K. Hencken, Phys. Rev. C **56**, 3054 (1997).
 - [15] L.-B. Wang *et al.*, Phys. Rev. Lett. **93**, 142501 (2004).
 - [16] G. Ewald *et al.*, Phys. Rev. Lett. **93**, 113002 (2004).
 - [17] A. Cobis, D. V. Fedorov, and A. S. Jensen, Phys. Rev. Lett. **79**, 2411 (1997).
 - [18] S. C. Pieper (private communication).
 - [19] B. S. Pudliner, V. R. Pandharipande, J. Carlson, and R. B. Wiringa, Phys. Rev. Lett. **74**, 4396 (1995).
 - [20] H. Esbensen and G. F. Bertsch, Nucl. Phys. **542**, 310 (1992).
 - [21] H. Esbensen and G. F. Bertsch, Phys. Rev. C **46**, 1552 (1992).
 - [22] K. Hagino and H. Sagawa, Phys. Rev. C **72**, 044321 (2005).
 - [23] M. Puchalski, A. M. Moro, and K. Pachucki, Phys. Rev. Lett. **97**, 133001 (2006).
 - [24] I. Tanihata *et al.*, Phys. Rev. Lett. **55**, 2676 (1985).
 - [25] J. A. Tostevin and J. S. Al-Khalili, Nucl. Phys. A **616**, 418c (1997).
 - [26] K. Varga, Y. Suzuki, and R. G. Lovas, Phys. Rev. C **66**, 041302(R) (2002).
 - [27] T. Myo, K. Kato, H. Toki, and K. Ikeda, Mod. Phys. Lett. **A21**, 2491 (2006).